Science of the Total Environment 618 (2018) 569–578

Contents lists available at ScienceDirect

Science of the Total Environment

journal homepage: www.elsevier.com/locate/scitotenv

Estimation of different source contributions to sediment organic matter in an agricultural-forested watershed using end member mixing analyses based on stable isotope ratios and fluorescence spectroscopy

Morgane Derrien [a], Min-Seob Kim [b], Giyoung Ock [c], Seongjin Hong [d], Jinwoo Cho [a], Kyung-Hoon Shin [e,*], Jin Hur [a,*]

[a] Department of Environment and Energy, Sejong University, Seoul 143-747, South Korea
[b] Environmental Measurement & Analysis Center, National Institute of Environmental Research, Incheon 22689, South Korea
[c] National Institute of Ecology, Seocheon 33657, South Korea
[d] Department of Ocean Environmental Sciences, Chungnam National University, Daejeon, 34134, South Korea
[e] Department of Marine Sciences and Convergent Engineering, Hanyang University, Ansan, Gyeonggi do 15588, South Korea

HIGHLIGHTS

- Different sources samples were characterized using fluorescence and stable isotopes.
- Relative source contributions of SeOM were estimated by EMMA.
- The results of EMMAs were compared with isotope versus fluorescence parameters.
- Inability of AEOM of sediments to represent original bulk POM was highlighted.

GRAPHICAL ABSTRACT

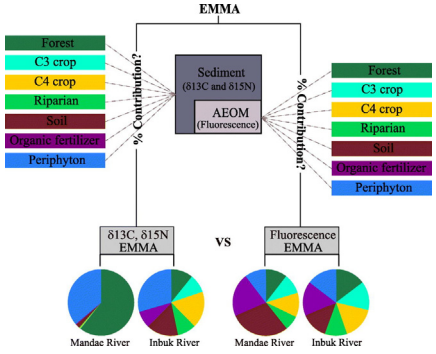

ARTICLE INFO

Article history:
Received 30 September 2017
Received in revised form 3 November 2017
Accepted 7 November 2017
Available online xxxx

Editor: Jay Gan

Keywords:
Sediment organic matter
EEM-PARAFAC
Stable isotope ratios
Source tracing
End-member mixing analysis

ABSTRACT

The two popular source tracing tools of stable isotope ratios ($\delta^{13}C$ and $\delta^{15}N$) and fluorescence spectroscopy were used to estimate the relative source contributions to sediment organic matter (SeOM) at five different river sites in an agricultural-forested watershed (Soyang Lake watershed), and their capabilities for the source assignment were compared. Bulk sediments were used for the stable isotopes, while alkaline extractable organic matter (AEOM) from sediments was used to obtain fluorescent indices for SeOM. Several source discrimination indices were fully compiled for a range of the SeOM sources distributed in the catchments of the watershed, which included soils, forest leaves, crop (C3 and C4) and riparian plants, periphyton, and organic fertilizers. The relative source contributions to the river sediment samples were estimated via end member mixing analysis (EMMA) based on several selected discrimination indices. The EMMA based on the isotopes demonstrated that all sediments were characterized by a medium to a high contribution of periphyton ranging from ~30% to 70% except for one site heavily affected by forest and agricultural fields with relatively high contributions of terrestrial materials. The EMMA based on fluorescence parameters, however, did not show similar results with low contributions from forest leaf and periphyton. The characteristics of the studied watershed were more consistent with the source contributions determined by the isotope ratios. The discrepancy in the EMMA capability for source

* Corresponding authors.
E-mail addresses: shinkh@hanyang.ac.kr (K.-H. Shin), jinhur@sejong.ac.kr (J. Hur).

https://doi.org/10.1016/j.scitotenv.2017.11.067
0048-9697/© 2017 Elsevier B.V. All rights reserved.

assignments between the two analytical tools can be explained by the limited analytical window of fluorescence spectroscopy for non-fluorescent dissolved organic matter (FDOM) and the inability of AEOM to represent original bulk particulate organic matter (POM).

© 2017 Elsevier B.V. All rights reserved.

1. Introduction

Sediments operate as sources and sinks of nutrients and pollutants in aquatic ecosystems. They store a large amount of organic carbon, acting as a dominant site for organic matter (OM) breakdown and nutrient regeneration (Burone et al., 2003; Ruddy, 1997). They are considered as an archive of past environmental conditions and biogeochemical processes in the surrounding areas (Torres et al., 2012). Sources of OM in aquatic sediments are multiple and diverse. The two major classified sources are (i) allochthonous sources such as materials from land (e.g., plants or soils) and/or upper catchment ecosystems, including also sources from anthropogenic activities (e.g., organic fertilizer, effluents from wastewater treatment facilities) and (ii) autochthonous such as OM derived from biota (e.g., algae, bacteria, plankton, and macrophytes) (Derrien et al., 2015). Identifying the origins of the OM in sediments provides a deep understanding of the dynamics of sediment organic matter (SeOM) and its role as a source of energy and nutrients in aquatic systems, as well as the distributions of contaminants and eutrophication processes (Dunn et al., 2008). It can also facilitate and improve the decision making regarding water management if SeOM can be related to a potential threat to drinking water and/or aquatic ecosystems (Derrien et al., 2017b).

Widely utilized tools to identify the OM origins, are stable carbon and nitrogen isotopes and fluorescence spectroscopy (Coble, 2007; Lambert et al., 2011; Xiao and Liu, 2010; Yang and Hur, 2014). Stable isotope ratios ($\delta^{13}C$ and $\delta^{15}N$) have been considered the most effective method of tracking both the sources and the transformation processes of organic matter (Toming et al., 2013). Physical, chemical or biological processes in natural environments can lead to changes in the isotopic composition due to a difference in atomic mass between ^{12}C and ^{13}C. For instance, according to the types of plants (e.g., C3, C4 or crassulacean acid metabolism (CAM)) and/or their specific photosynthetic paths, the isotopic ratios may subject to change. C3 presents the values between −33 to −24‰, while the values range from −16 to −10‰ for C4 and between −20 and −10‰ for CAM. Several studies demonstrated the strong capability of the carbon isotope ratios to distinguish between allochthonous and autochthonous origins (Amiotte-Suchet et al., 2007; Benner et al., 1997; Lambert et al., 2011; Lehmann et al., 2002; Meyers, 1994; Toming et al., 2013). The use of nitrogen stable isotopes for source discrimination is limited due to very complex geochemical cycling of nitrogen and the involvement of many species in the nitrogen pool (inorganic and organic forms) (Bianchi and Canuel, 2011). However, the combined use of nitrogen and carbon stable isotopes enables effective source tracing of particulate OM (POM) (Barros et al., 2010; Gao et al., 2012; Graham et al., 2001; Ogrinc et al., 2005).

Fluorescence spectroscopy has also been widely used to trace OM sources especially using water- or alkali-extractable OM (WEOM or AEOM) from soils and sediments (Coble, 2007; Derrien et al., 2017a; He et al., 2016b; Osburn et al., 2012; Santín et al., 2009). A fraction of the OM, named FDOM, can emit fluorescence after absorbing UV–Visible light. The investigation of the spectroscopic characteristics allows to distinguish different fluorescent components, and helps to identify the types of sources of samples due to a large variability of the characteristics affected by their origins. Many optical indices can be derived from fluorescence spectroscopy, and their capabilities for source identification have been tested in many aquatic environments such as wastewater, rivers, groundwater, lakes, rainwater, and oceans (Derrien et al., 2017b; Fichot et al., 2013; Hur et al., 2006; Inamdar et al., 2011). Meanwhile, fluorescence excitation emission matrices combined with parallel factor analysis (EEM-PARAFAC) could provide alternative indices for OM sources by using the relative abundances or the relative ratios of different independent fluorescent components, which are decomposed from the EEM datasheet of bulk samples (Stedmon and Bro, 2008; Stedmon et al., 2003).

Although the spectroscopic methods have provided reliable tools to trace the source of organic matter in many previous literatures, they also revealed limited analytical window, which might lower their efficiency, especially, in a complex and mixed environment (Derrien et al., 2017b; Goncalves-Araujo, 2016; Schindler Wildhaber et al., 2012; Yang and Hur, 2014). The Soyang Lake watershed is the largest reservoir system of South Korea. It is located in the upstream region of the Han River (Fig. 1), which serves as the main source of drinking water for about 23 million people of South Korea (Lee et al., 2016). The watershed has a total area of 2700 km^2 with the altitude range from 80 to 1700 m (Jung et al., 2015; Tenhunen et al., 2011). Approximately 85% of the catchment is covered with forest, 7% is used intensely as arable land (including crops of radishes, cabbages, ginseng, corn, potatoes, and paddy fields) and another 7% as residential area (Choi et al., 2010; Lee et al., 2013). The steep slopes of the watershed facilitate an extremely high transport of POM from various potential sources especially during summer Monsoon season (e.g., annual precipitation of 1370 mm, with 70% of it occurring from late June to September (Arnhold et al., 2014; Tenhunen et al., 2011)). Therefore, sediments in this watershed can be viewed as an interesting location to explore the source discrimination capabilities of various indices.

The overall goal of the study was to compare fluorescence and stable carbon and nitrogen isotopes for assessing their relative contributions to river sediments with the carbon sources within a drainage-basin. For this, several source tracing indices were compiled for many potential SeOM sources, which include soils, forest, crop (C3 and C4), riparian plants, periphyton, and organic fertilizers. To the best knowledge of the authors, this is the first study applying both techniques on similar sourced samples. The relative contributions of different OM sources to the river SeOM samples in Soyang Lake watershed were estimated via end member mixing analysis based on the compiled indices.

2. Materials and methods

2.1. Study area and sampling

Sampling for OM sources and sediments was in May 2015. The source materials were chosen considering that the upstream catchments are mostly forested and agricultural lands. Forest leaves, C3 and C4 crop plants, riparian plants, soil, and organic fertilizer were collected as the OM allochthonous sources from forested areas, river banks and/or agricultural fields. Periphyton (e.g., autochthonous source) was collected from the river beds of the Inbuk and Buk streams since the plankton could be a major source of POM in storm events (Hur et al., 2014). In total, 36 source samples, representing 7 different sources, were collected in the field (Table S1). Five surface sediment samples were collected using a grab sampler (Ekman dredge) in 4 different major tributaries of the Soyang Lake watershed: Mandae River (MD), Inbuk River (IBa and IBb), Buk River (B) and Soyang River (S) (Fig. 1). At the laboratory, the source and sediment samples were stored at −20 °C. They were freeze-dried and grinded for further analyses. Branches and leaves were removed from soils before grinding.

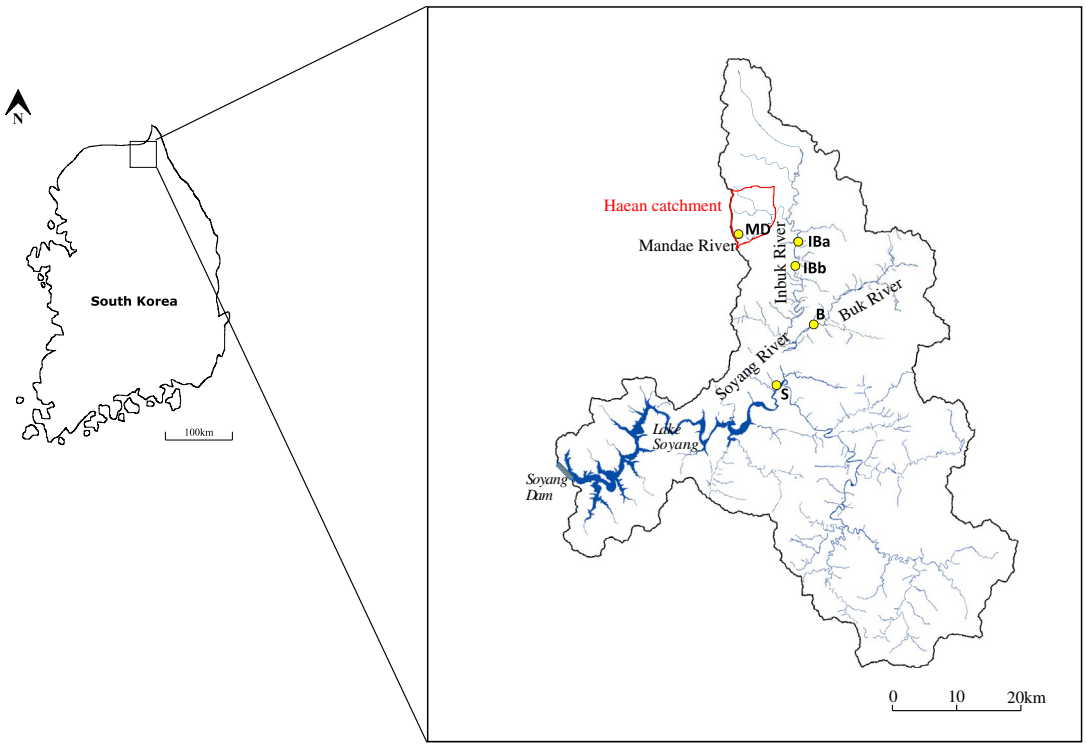

Fig. 1. Map of Soyang Lake watershed with six sampling locations indicated by yellow-colored circles (i.e., MD: Mandae River; IBa,b: Inbuk River, B: Buk river; S: Soyang River). The border of Haean basin are underlined in red. (For interpretation of the references to color in this figure legend, the reader is referred to the web version of this article.)

2.2. Carbon and nitrogen stable isotope ratio analyses

Before carbon stable isotope analysis, inorganic carbon was removed by 1 N HCl treatment, whereas untreated samples were directly used for the nitrogen isotope ratio analysis (Carabel et al., 2006). Stable carbon and nitrogen isotope ratios of the samples were measured using an elemental analyzer coupled with an isotope ratio mass spectrometer (EA-IRMS; EuroEA-Isoprime IRMS, GV Instruments, UK). Stable isotope ratios were calculated using the standard δ notation:

$$X(‰) = \left(\left(R_{sample}/R_{Reference}\right) - 1\right) \times 1000 \quad (1)$$

where, X = C (carbon) or N (nitrogen), and R is the corresponding ratio of $^{13}C/^{12}C$ or $^{15}N/^{14}N$. The standard reference materials were Vienna Pee Dee Belemnite (VPDB) for carbon and atmospheric N_2 for nitrogen. The analytical precision was 0.05‰ and 0.1‰ for carbon and nitrogen, respectively.

2.3. Measurements of absorption and fluorescence spectra

Alkaline extractable organic matter (AEOM) was obtained based on (Derrien et al., 2017a). Briefly, the ground samples were soaked in 0.1 N NaOH at a solid-to-liquid mixing ratio of 1:10, and shaken for 24 h before centrifugation (5000 rpm for 20 min) and subsequent filtration through a pre-washed 0.45μm pore-sized membrane (cellulose acetate, Toyo Roshi Kaisha, Ltd., Japan). The filtrate was finally passed through cation exchange resin (Dowex 50WX8-100, Sigma).

Absorption spectra were scanned from 200 to 800 nm at 1 nm-interval using an ultraviolet-visible (UV–Vis) spectrometer (Shimadzu UV-1300). Fluorescence EEMs were scanned on a luminescence spectrometer (Hitachi F7000, Japan) with the excitation wavelengths (Ex) stepping from 220 to 500 nm at 5 nm-increment, and the emission wavelengths (Em) from 280 to 550 nm at 1 nm-intervals. Both slit widths were set to 10 nm, and the scanning speed was 12,000 nm/min. Blank subtraction and Raman peak normalization were performed following the procedures proposed by (Murphy et al., 2010). Before the EEM measurements, the samples were sufficiently diluted with distilled and deionized water (DDW) until the UV absorbance at 254 nm was below 0.05 cm^{-1} (Hur et al., 2009) to avoid the inner-filter correction. The pH was fixed at 3.0 for fluorescence measurements to minimize the potential interferences from metal presence. A total of 41 EEMs were collected for PARAFAC modeling. The number of different fluorescent components was determined based on the split-half validation and Tucker's congruence coefficients (>0.95) (Table S2). The procedure is well described in the protocol suggested by (Stedmon and Bro, 2008). The modeling was carried out in MATLAB R2013b (Mathworks, USA) with the DOMFluor toolbox (www.models.life.ku.dk). The maximum fluorescence intensities (F_{max}) of identified components were used to represent their relative abundance (%) and different ratios.

Fluorescence index (FI), humification index (HIX), and biological index (BIX) were calculated as fluorescence-based source discrimination indicators. FI, a proxy of aquatic humic substances sources (i.e., microbial versus terrestrial sources), was measured using the ratio of the emission intensity at 450 nm to that at 500 nm at Ex of 370 nm (McKnight et al., 2001). The humification index (HIX), an indicator for the degree of DOM humification, was estimated using the ratio of the areas under the emission spectra over 435–480 nm to 300–345 nm at Ex of 255 nm (Zsolnay et al., 1999). The biological index (BIX), an index of the recent autochthonous and biological contribution, was calculated by the ratio of the fluorescence intensity at the Em of 380 nm to 430 nm at 310 nm (Ex) (Huguet et al., 2009).

2.4. End member mixing analysis (EMMA) using isotope ratios and fluorescent indicators

The potential contribution of selected OM sources to the river sediments were estimated using the freeware package IsoSource version 1.3.1. This software calculates the proportions of different end members in the mixture via an isotopic mass balance equation (http://www.epa.

gov/eco-research/stable-isotope-mixing-models-estimating-source-proportions) (Phillips and Gregg, 2003; Phillips et al., 2005). In the present study, this software was applied to the results from both the isotope ratio and fluorescence analyses.

First, end member mixing analysis (EMMA) models were constructed using five to seven end-members and the two stable isotope ratios ($\delta^{13}C$ and $\delta^{15}N$). Based on the rules suggested in Phillips et al. (2005), some sources were combined (e.g., C3 crop and riparian plant) and one end member had to be removed in some cases. The source increment and mass balance tolerance parameter values were fixed at 1% and 0.01‰, respectively, for the samples from the Inbuk River (IBa and IBb). Different mass balance tolerance values were applied to the other sites (0.5 ‰ for MD and 2‰ for B and S samples) because no statistics were generated at the setting with the lowest value (0.01‰). The modification in the mass balance tolerance does not likely affect the EMMA results. For example, Phillips and Gregg (2003) demonstrated no significant changes in the medians of the distributions of the possible source contributions by the alterations of the mass balance tolerance.

In the last step, the fluorescence parameters applicable for the EMMAs were selected according to the two considerations outlined below.

(i) For all the possible fluorescence parameters from relative abundances and the relative ratios of FDOM components, and three fluorescent indicators, the value ranges between the sediment and the end-member samples were compared, and the parameters of sediments exceeding the end-member ranges were removed (Yang et al., 2015). In this procedure, the number of parameters was reduced to 8 (e.g., %C2, FI, HIX, C1/C3, C2/C1, C3/C1, C4/C2, and C5/C4).

(ii) Several pairs of parameters were selected with each representing contrasting sources (e.g., allochthonous versus autochthonous). HIX and C3/C1 corresponded to allochthonous sources, while %C2 and C2/C1 relate to autochthonous sources. Finally, four fluorescent indicators (i.e., %C2, HIX, C3/C1, and C2/C1) were selected for the EMMA. The source increment was 2%, and the value for mass balance tolerance was set at 1‰ for all sediments. All the models based on the fluorescence parameters were performed with all 7 different sources.

3. Results and discussion

3.1. $\delta^{13}C$ and $\delta^{15}N$ on bulk samples

The measured values of $\delta^{13}C$ and $\delta^{15}N$ for the source and the sediment samples are presented in Table 1. These results are also illustrated in the end-member plot of $\delta^{15}N$ versus $\delta^{13}C$ (Fig. 2). For the source samples, the values of $\delta^{13}C$ and $\delta^{15}N$ ranged from -29.08 ± 1.58‰ to -17.02 ± 0.85‰ and from -1.37 ± 1.11‰ to 10.72 ± 0.21‰, respectively. The low levels of $\delta^{13}C$ corresponded to all the C3 plants (including crop plants, forest leaves, and riparian plants), while C4 crop had the highest value. A similar observation was reported in the literature, with the values ranging from −35‰ to 21‰ for C3 plants and −15‰ to −9‰ for C4 plants (Briggs et al., 2013; Yoon et al., 2016). The values for soil samples agreed with those from other soils (e.g., -24.53 ± 1.65‰) (Fig. 2) (Lambert et al., 2011; Yu et al., 2015). The $\delta^{13}C$ values for organic fertilizer (e.g., -25.90 ± 0.56‰) were between those of soils and C3 crop (Fig. 2) and are similar to those of sludge samples (Lee et al., 2014). The periphyton samples average -17.02 ± 0.85‰, which was close to the values of microalgae or land-based C4 and C4 salt marsh plants (Briggs et al., 2013; McCallister et al., 2004). The different sources were discriminated to a greater extent by using the $\delta^{15}N$ results. For example, the lowest $\delta^{15}N$ values were observed for forest leaves (e.g., -1.37 ± 1.11‰), followed by soil (e.g., 2.45 ± 2.14‰) and periphyton (e.g., 4.17 ± 1.35‰). By contrast, organic fertilizer and C4 crop showed relatively high $\delta^{15}N$ values of 9.22 ± 3.38‰ and 10.72 ± 0.21‰, respectively. The relatively large standard deviation of the $\delta^{15}N$ for the organic fertilizer samples is attributed to the differences in the composition because the source samples vary from raw manure to transformed manure, and vegetal residues (Table S1). The $\delta^{15}N$

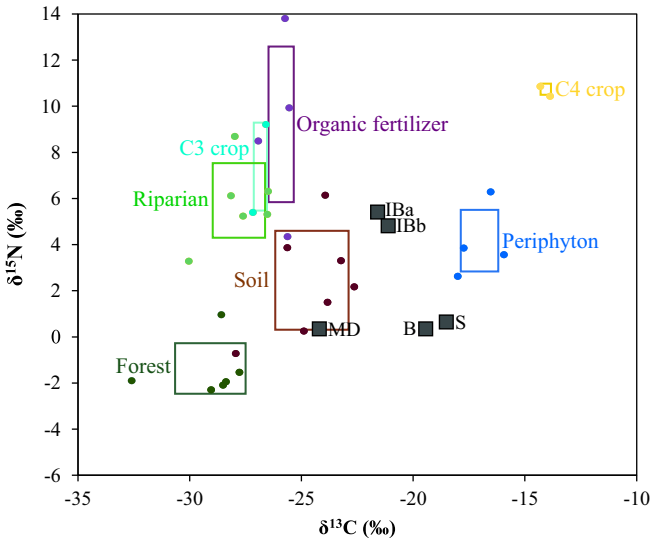

Fig. 2. Plot of $\delta^{13}C$ versus $\delta^{15}N$ for all the source end members and sediment samples (i.e., MD: Mandae River; IBa,b: Inbuk River, B: Buk river; S: Soyang River). The colored rectangles represent the standard deviations of the average value of each end-member. (For interpretation of the references to color in this figure legend, the reader is referred to the web version of this article.)

Table 1
Average distribution and standard deviation of the relative concentrations (%) of the 5 identified components (%) and carbon and nitrogen stable isotopic ratios (‰) for the source and sediment samples.

		Stable isotope ratios		Fluorescence parameters							
	Samples	$\delta^{13}C$ (‰)	$\delta^{15}N$ (‰)	C1 (%)	C2 (%)	C3 (%)	C4 (%)	C5 (%)	FI	HIX	BIX
Sources	Forest leaf ($n = 6$)	-29.08 ± 1.58	-1.37 ± 1.11	21.4 ± 5.5	36.2 ± 9.3	27.0 ± 6.9	7.0 ± 4.0	8.4 ± 4.3	1.2 ± 0.2	4.5 ± 1.5	0.4 ± 0.1
	C3 crop plant ($n = 2$)	-26.82 ± 0.29	7.38 ± 1.90	13.1 ± 0.4	37.3 ± 4.2	37.1 ± 4.9	9.5 ± 1.3	3.0 ± 0.2	1.1 ± 0.1	1.8 ± 0.3	0.3 ± 0.0
	C4 crop plant ($n = 2$)	-14.06 ± 0.22	10.72 ± 0.21	23.2 ± 7.7	34.6 ± 8.3	27.6 ± 1.3	7.0 ± 3.4	7.7 ± 2.7	1.1 ± 0.0	4.3 ± 2.5	0.4 ± 0.0
	Riparian plant ($n = 11$)	-27.76 ± 1.21	5.91 ± 1.61	13.0 ± 5.7	42.8 ± 10.5	27.8 ± 11.0	13.7 ± 7.2	2.7 ± 1.4	1.1 ± 0.1	1.7 ± 0.9	0.5 ± 0.3
	Soil ($n = 7$)	-24.53 ± 1.65	2.45 ± 2.14	38.0 ± 3.7	20.0 ± 6.4	21.3 ± 4.8	14.9 ± 3.7	5.7 ± 1.0	1.1 ± 0.1	7.5 ± 1.6	0.5 ± 0.1
	Organic fertilizer ($n = 4$)	-25.90 ± 0.56	9.22 ± 3.38	28.6 ± 8.6	27.8 ± 11.9	21.8 ± 4.0	13.8 ± 1.9	7.9 ± 1.3	1.4 ± 0.1	5.9 ± 3.7	0.6 ± 0.2
	Periphyton ($n = 4$)	-17.02 ± 0.85	4.17 ± 1.35	27.3 ± 9.5	36.4 ± 9.3	14.2 ± 4.4	16.0 ± 0.9	6.1 ± 2.5	1.2 ± 0.1	6.0 ± 4.2	0.8 ± 0.1
Sediment	Mandae River (MD)	−24.15	0.36	26.9	30.0	25.5	10.5	7.1	1.2	5.2	0.4
	Inbuk River a (IBa)	−21.56	5.33	14.1	33.3	11.1	23.4	18.0	1.2	2.1	1.1
	Inbuk River b (IBb)	−21.13	4.86	18.6	29.3	17.2	22.7	12.1	1.2	2.6	1.0
	Buk River (B)	−19.37	0.30	9.9	37.3	12.1	20.9	19.7	1.2	2.0	1.2
	Soyang River (S)	−18.50	0.72	17.7	32.6	16.3	22.0	11.5	1.2	2.4	0.9

values for the different sources agreed with literature (Briggs et al., 2013; Xiao and Liu, 2010).

The isotope ratios for all sediment samples remained within the limits for the end member sources (Fig. 2), suggesting that the sources of SeOM can be constrained by the collected end members. As expected from the similar sampling locations, both Inbuk (IB) river sediments had similar isotope ratios with the $\delta^{13}C/\delta^{15}N$ pair of −21.56‰/5.33‰ for IBa and −21.13‰/4.86‰ for IBb (Table 1). Buk (B) and Soyang (S) River sediments also showed similar isotope ratios probably due to their close locations. The isotope ratio pair of Mandae sediment sample was within the soil end member (Fig. 2), suggesting that soils can be the main SeOM source for the sediment.

3.2. Fluorescence analyses on AEOM

3.2.1. Identification of fluorescent components from EEM-PARAFAC

Five components were identified, of which three humic-like components (C1, C3, and C5) and two protein-like component (C2 and C4) (Fig. 3 and Table S2). All the identified components were consistent with those previously reported and/or well-matched with the Open Fluor database with similarity scores of >0.950. Component 1 (C1) with the Ex/Em maxima at 225, 340/434 nm can be assigned to the typical humic-like component (Guéguen et al., 2014; Jørgensen et al., 2011), while the component 5 (C5) (peaks at 240, 275, 355/470 nm) can be assigned to a humic-like component and probably to a mixture of peak A and C not well separated by the PARAFAC analysis as we observed an atypical 'three-peak pattern' for this component (Yamashita et al., 2013). Component 3 (C3), exhibiting the peaks at 220, 310/434 nm, can be associated with terrestrial humic substances (Stedmon and Markager, 2005; Williams et al., 2010). Component 2 (C2) (peak at 220, 270/326 nm (Ex/Em)) and 4 (C4) (peak at 220–285/368 nm) has been reported as protein-like or tryptophan-like fluorophores with a microbial-produced origin and possibly derived from aquatic production (Graeber et al., 2012; Williams et al., 2010).

3.2.2. Relative abundance of fluorescent components and fluorescence indices

The relative abundance of the fluorescent components was calculated by the ratio of each component over the sum of the F_{max} values of all five components. Components C1, C2, and C3 exhibited relatively higher abundances than C4 and C5 although a range of variations were found among the sources (Table 1 and Fig. 4a). The protein-like component C2 was the most dominant for all end member sources (e.g., 34.6 ± 8.3 to 42.8 ± 10.5%) except for organic fertilizer and soil samples (e.g., 27.8 ± 11.9 and 20.0 ± 6.4%, respectively). C1 was the most abundant component in soil and organic fertilizer (e.g., 38.0 ± 3.7% for soils and 28.6 ± 8.6% for organic fertilizers), while it represented the second and the third most abundant component in periphyton (e.g., 27.3 ± 9.5) and plant samples (e.g., values ranged from 13.0 ± 5.7 to 23.2 ± 7.7), respectively. The terrestrial humic-like component (C3) was the second most abundant component in all the plant samples (e.g., forest leaf, C3 and C4 crop plants, and riparian plants). Among the sources, the highest relative abundances of C4 were observed in the periphyton and riparian plant samples (>13.5%).

Regarding the fluorescent indicators from EEMs, the FI values of all samples ranged from 1.1 to 1.4 (Table 1), exhibiting the typical characteristics of terrestrial materials (McKnight et al., 2001). The sediment samples did not exhibit any variations, with a fixed value of 1.2.

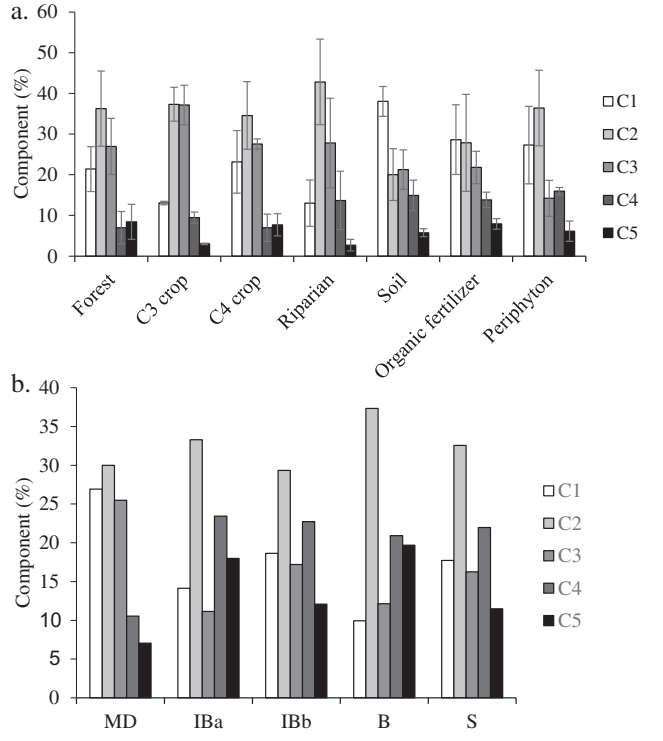

Fig. 4. Distribution of the 5 fluorescent components identified by EEM-PARAFAC for the sources samples (a) and the sediment samples (b) (i.e., MD: Mandae River; IBa,b: Inbuk River, B: Buk river; S: Soyang River). C1: Humic-like material with microbial activity; C2: Protein-like or tryptophan-like component; C3: Terrestrial humic-like; C4: Humic-like material, possible phytoplankton-derived, labile material; C5: Fulvic acid-like, microbially transformed.

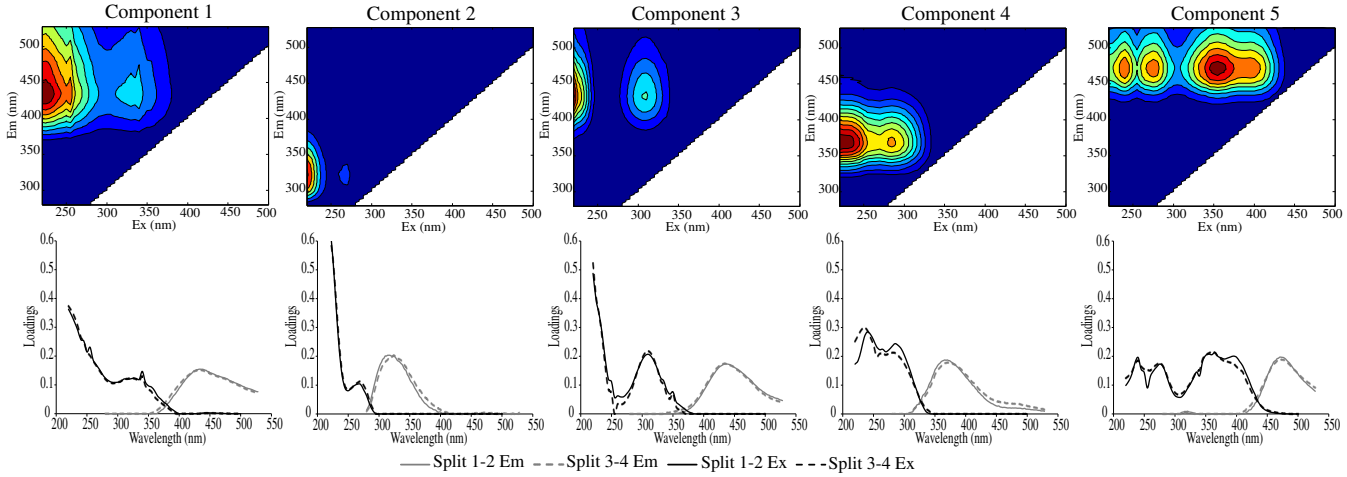

Fig. 3. Contour plots of five fluorescent components identified from EEM-PARAFAC. The emission (Em) and the excitation (Ex) loading are shown for the first and the second split-half.

Meanwhile, the source samples presented the average HIX values from 4.3 to 7.5, representing weakly humified terrestrial materials. Relatively high HIX values (e.g., 6.0 ± 4.2) were unexpectedly observed for the periphyton source (e.g., 7.5 ± 1.6). The C3 crop and riparian plant samples presented relatively low HIX values (1.8 ± 0.3 and 1.7 ± 0.9, respectively). A limited range of the BIX values were observed among the different source samples, while those of the sediment samples exceeded the ranges of the end member sources, suggesting the application limitation for source discrimination. Of the three fluorescent indicators, HIX is thus likely to be the only indicator applicable for source apportionment.

Among the sediment samples, MD presented the unique fluorescence characteristics distinguished from others (Table 1 and Fig. 4b). It was characterized by the high abundance of the two terrestrial humic-like components (e.g., C1 and C3, 26.9 and 25.5%, respectively) and the protein-like component (C2, 30.0%). This sample also exhibited the highest HIX value (5.2). The combined results revealed that the MD sediment could be heavily affected by allochthonous organic matter. The distribution of the fluorescent components and the values of the indices suggest the existence of a substantial input from forest leaves and soil sources.

3.3. End member mixing analyses (EMMA)

The relative contribution of each OM source to the five river sediments was estimated using IsoSource software (Phillips, 2001) based on the analyses of fluorescence and stable isotope ratios. Although this software is most commonly practiced with stable isotope ratios, its use is not restricted to the isotope ratios as the software was built based on a mass balance equation.

3.3.1. EMMA with $\delta^{13}C$ and $\delta^{15}N$

The most important factor in the uncertainty in the estimates of source contributions is the degree of the dissimilarity in the isotope ratios (or end member values) between different sources. The sources must have isotopically distinct signatures (Phillips et al., 2014; Phillips et al., 2005). In the same literature, it was stated that if a source is inside the convex polygon bounded by all other sources in the plot of $\delta^{13}C$ versus $\delta^{15}N$, this end member may not contribute to the model (Phillips and Gregg, 2003). It was observed in Fig. 2 that the C3 crop and the riparian plants overlapped with each other, which is not surprising as riparian plants are C3 plants. Another point to note regarding the plot of $\delta^{13}C$ versus $\delta^{15}N$ is the location of the soil end-member inside the polygon created by the other sources. Based on the rules suggested in Phillips et al. (2005), it may be necessary to combine the C3 crop and riparian plant and also to remove the soil end-member from the model. Four different models were tested with the number of end-members varying from 5 to 7 (Table 2), which included a model excluding soil and combining C3 crop and the riparian plant as end members (e.g., Model 1), two models with 6 end-members (e.g., one combining C3 crop and riparian plant (Model 2), and one without soil (Model 3)), and the last model with 7 end-members including the soil source (Model 4). As soil is most important component in the OM contribution in sediment in Korea (Tenhunen et al., 2011), this end member was kept for some models of the EMMA (i.e., Model 2 and 4). It is a common observation that soil particles are easily eroded and transported into rivers during intense storm events (Jung et al., 2014).

From the results of the 4 different models, two distinctive trends of the source contributions were observed among the sediments (i.e., MD, B, and S versus IBa and IBb). No significant differences in the percent contribution of each source were found among the two groups of samples (e.g., p-values > 0.998). Furthermore, in the models including the soil end-member (Model 2 and 4), the IBa and IBb sediments showed a significant soil contribution (~15.0%) (Table 2). This suggests that it may not be a strict constraint for the estimation whether or not to include the source (i.e., soil). Phillips et al. (2014) explained that the decision on source grouping or the exclusion of sources should not be strictly made by standard rules. In addition, although the data of the C3 crop plant and the riparian plant sources overlapped in the plot of

Table 2
Relative contributions to sediment samples estimated from 4 different models using $\delta^{13}C$ and $\delta^{15}N$. For each sample, mean, minimum, maximum, standard deviation (sd) of the calculated contributions are presented. Model 1: 5 end-members (e.g., forest leaf, C3 crop combined with riparian plant, C4 crop plant, organic fertilizer, and periphyton), Model 2: 6 end-members (e.g., all sources with combination of the C3 crop and riparian plant end-member), Model 3: 6 end-members (all sources minus soil end-member), Model 4: 7 end-members (e.g., all studied sources).

Model	End-member	Contribution (%)									
		MD (1‰, 0.5‰)		IBa (1‰, 0.01‰)		IBb (1‰, 0.01‰)		B (1‰, 2‰)		S (1‰, 2‰)	
		Mean ± sd	Range	Mean ± sd	Range	Mean ± sd	Range	Mean ± sd	Range	Mean ± sd	Range
1	Forest leaf	61.6 ± 0.8	60–63	18.8 ± 10.5	4–41	21.1 ± 9.1	7–39	35.3 ± 0.7	34–36	27.9 ± 0.8	27–29
	C3 crop/riparian plant	0.4 ± 0.5	0–2	17.4 ± 10.5	0–36	11.2 ± 8.8	0–29	0.0 ± 0.4	0–1	0.4 ± 0.7	0–2
	C4 crop plant	0.5 ± 0.7	0–2	19.3 ± 12.8	1–47	17.0 ± 11.2	0–41	0.0 ± 0.8	0–2	0.6 ± 0.7	0–2
	Organic fertilizer	0.2 ± 0.4	0–1	11.3 ± 7.7	0–28	10.0 ± 6.9	0–24	0.0 ± 0.4	0–1	0.1 ± 0.3	0–1
	Periphyton	37.3 ± 1.2	35–40	33.3 ± 14.4	2–54	40.8 ± 12.6	14–60	64.0 ± 1.2	62–66	71.0 ± 1.2	69–73
2	Forest leaf	60.5 ± 1.4	57–63	12.8 ± 9.6	0–41	12.7 ± 9.2	0–43	34.5 ± 1.1	32–36	27.0 ± 1.1	25–29
	C3 crop/riparian plant	0.3 ± 0.5	0–2	12.0 ± 8.8	0–39	9.4 ± 7.7	0–36	0.1 ± 0.3	0–1	0.3 ± 0.5	0–2
	C4 crop plant	0.5 ± 0.7	0–3	21.0 ± 11.9	0–48	16.9 ± 10.4	0–47	0.4 ± 0.6	0–2	0.4 ± 0.6	0–2
	Soil	2.4 ± 2.4	0–10	18.4 ± 11.9	0–62	18.3 ± 13.6	0–64	1.5 ± 1.7	0–6	1.6 ± 1.7	0–6
	Organic fertilizer	0.2 ± 0.4	0–1	10.9 ± 7.4	0–35	7.9 ± 6.3	0–27	0.1 ± 0.3	0–1	0.1 ± 0.3	0–1
	Periphyton	31.6 ± 1.6	33–40	24.9 ± 13.3	0–55	34.7 ± 13.3	5–60	63.5 ± 1.1	62–66	70.7 ± 1.2	68–73
3	Forest leaf	61.6 ± 0.8	60–63	16.0 ± 9.6	0–41	17.2 ± 8.6	2–45	35.1 ± 0.7	34–60	27.8 ± 0.7	27–29
	C3 crop plant	0.3 ± 0.5	0–2	10.9 ± 8.8	0–39	8.5 ± 6.9	0–30	0.1 ± 0.3	0–1	0.3 ± 0.5	0–1
	C4 crop plant	0.4 ± 0.7	0–2	16.1 ± 11.9	0–49	13.4 ± 10.5	0–48	0.4 ± 0.7	0–2	0.5 ± 0.7	0–2
	Riparian plant	0.3 ± 0.6	0–2	11.5 ± 9.0	0–44	9.4 ± 7.6	0–34	0.2 ± 0.4	0–1	0.3 ± 0.7	0–2
	Organic fertilizer	0.2 ± 0.4	0–1	8.7 ± 7.4	0–34	6.6 ± 5.9	0–24	0.1 ± 0.3	0–1	0.1 ± 0.3	0–1
	Periphyton	37.2 ± 1.2	35–40	36.7 ± 13.3	0–55	44.9 ± 11.8	6–61	64.1 ± 1.1	62–66	71.0 ± 1.1	69–73
4	Forest leaf	60.6 ± 1.3	57–63	10.8 ± 8.5	0–41	10.8 ± 8.0	0–45	34.4 ± 1.0	31–36	27.0 ± 1.1	25–29
	C3 crop plant	0.2 ± 0.4	0–2	9.0 ± 7.5	0–40	7.1 ± 6.1	0–33	0.1 ± 0.3	0–1	0.2 ± 0.4	0–1
	C4 crop plant	0.4 ± 0.7	0–3	17.8 ± 10.6	0–49	13.2 ± 9.1	0–48	0.3 ± 0.6	0–2	0.3 ± 0.6	0–2
	Riparian plant	0.3 ± 0.5	0–2	9.1 ± 7.7	0–44	7.6 ± 6.6	0–36	0.1 ± 0.3	0–1	0.2 ± 0.5	0–2
	Soil	2.2 ± 2.3	0–10	15.6 ± 12.4	0–62	15.0 ± 11.6	0–64	1.3 ± 1.6	0–6	1.5 ± 1.6	0–6
	Organic fertilizer	0.1 ± 0.3	0–1	8.2 ± 6.7	0–35	6.2 ± 5.3	0–27	0.1 ± 0.3	0–1	0.1 ± 0.2	0–1
	Periphyton	36.2 ± 1.5	33–40	29.5 ± 13.5	0–55	40.0 ± 11.6	5–61	63.6 ± 1.1	62–66	70.7 ± 1.1	68–73

$\delta^{13}C$ versus $\delta^{15}N$, it may be inappropriate to combine the two end members in the modeling as the standard deviations of the sources were lower in model 4 (two separated sources) than in the model 2 (combined sources). Consequently, model 4 was finally selected for this study, and the estimated contributions were further discussed (Table 2).

The MD sediment was mainly characterized by the sources forest leaf and periphyton (Table 2). The SeOM of this river thus seems to be largely affected by a high terrestrial input from surrounding forests with a percentage of 60.6 ± 1.3% as well as by the autochthonous sources represented by periphyton (e.g., 36.2 ± 1.5%). The contributions of the other sources were minor (~2.3%). The MD river, an agricultural river draining the Haean Basin (Fig. 1), is located in an area covered by 60% forest, 24% upland fields and 8% of rice paddy fields (Arnhold et al., 2014; Kim et al., 2015). The input of terrestrial OM from Haean Basin into this river could be intensified by its mountainous topography (elevation of 400–1304 m) and annually by a strong episode of precipitation (Jung et al., 2015). The B and S sediments were also characterized by the two sources but with opposite trends: 34.4 ± 1.0% (forest leaf) and 63.6 ± 1.1% (periphyton) and 27.0 ± 1.1% (forest leaf) and 70.7 ± 1.1% (periphyton), respectively. The results of this study agreed with Namkung et al. (2001), who quantified the autochthonous organic matter in the same area to an average percentage of 53.6% over the year. By contrast, the two sediments of the Inbuk River (IBa and IBb) exhibited more complex contributions from diverse sources than the other river sediments. Although the main contribution was made by the autochthonous source (i.e., periphyton) with the percentages of 29.5 ± 13.5% and 40.0 ± 11.6% for IBa and IBb, respectively, the total terrestrial contributions to these samples reached 62.3 and 53.7% for IBa and IBb, respectively, with the higher contribution of C4 crop (e.g., 17.8 ± 10.6% and 13.2 ± 9.1%, respectively) and soil (e.g., 15.6 ± 12.4% and 15.0 ± 11.6%, respectively). Meanwhile, anthropogenic input (i.e., organic fertilizer) was also detected in these IB sediments with low contributions of 8.2 ± 6.7% and 6.2 ± 5.3% for IBa and IBb, respectively. The occurrence of anthropogenic OM can be explained by the transport of this material along Mandae, which is characterized by intensive agricultural activities in Haean Basin, into Inbuk followed by the accumulation in the IB sediments as the Mandae is a tributary of the Inbuk River.

3.3.2. EMMA with the pre-selected fluorescent indices

Four models have been performed based on the fluorescence parameters. The results of these models are presented in Table 3.

Models 5 (using C3/C1 and C2/C1) and 7 (using %C2 and HIX) showed similar source contributions. Model 6 using %C2 and HIX did not even generate the results for IBb. Model 8 (using HIX and C2/C1) presented similar source distribution to model 5 for B and to model 6 for MD. However, it presented notable differences in the source contributions for three other sediments. Except for the model 6 which failed to produce the result for IBb, model 7 (i.e., %C2 and C3/C1) was finally selected for this study because it presented the lowest standard deviation and ranges of values.

A similar distribution in the source contributions was observed for the MD and IBb sediments (Table 3). These samples were mainly characterized by the sources of soil (e.g., 29.2 ± 10.7% and 33.2 ± 10.7%, respectively) and organic fertilizer (e.g., 21.1 ± 17.7% and 20.6 ± 17.7%, respectively). The IBa and S sediments were characterized by nearly equal contributions from all sources without any predominant contributions. By contrast, the B sediment presented the unique characteristics in the source contributions with the lowest values from soil and organic fertilizer and the highest values from riparian plant (29.9 ± 13.2%).

The high contributions of soil and organic fertilizer reflect that this watershed includes an upstream catchment with intensive agricultural activity (e.g., Haean Basin) (Kim et al., 2015; Tenhunen et al., 2011). In

Table 3
Relative contributions to sediment samples estimated from 4 different models using fluorescence parameters. For each sample, mean, minimum, maximum, standard deviation (sd) of the calculated contributions are presented. Model 5: using C3/C1 and C2/C1. Model 6: using %C2 and HIX. Model 7: using %C2 and C3/C1. Model 8: using HIX and C2/C1.

Model	End-member	Contribution (%)									
		MD (2‰, 1‰)		IBa (2‰, 1‰)		IBb (2‰, 1‰)		B (2‰, 1‰)		S (2‰, 1‰)	
		Mean ± sd	Range	Mean ± sd	Range	Mean ± sd	Range	Mean ± sd	Range	Mean ± sd	Range
5	Forest leaf	15.1 ± 9.7	0–100	15.2 ± 13.7	0–100	14.9 ± 13.5	0–100	6.1 ± 8.5	0–58	14.9 ± 14.7	0–100
	C3 crop plant	11.3 ± 9.1	0–60	11.7 ± 9.9	0–52	12.6 ± 11.0	0–58	11.8 ± 9.9	0–54	11.9 ± 11.5	0–55
	C4 crop plant	15.3 ± 10.8	0–100	15.3 ± 13.8	0–100	14.9 ± 13.6	0–100	8.8 ± 8.2	0–56	14.9 ± 14.7	0–100
	Riparian plant	7.9 ± 6.9	0–44	12.4 ± 10.6	0–58	11.8 ± 10.1	0–58	49.8 ± 9.1	20–80	12.3 ± 11.9	0–65
	Soil	17.8 ± 10.7	0–100	14.2 ± 11.9	0–76	15.4 ± 13.5	0–98	5.3 ± 5.2	0–36	15.3 ± 14.6	0–90
	Organic fertilizer	16.7 ± 17.7	0–100	15.4 ± 13.6	0–96	15.2 ± 13.6	0–100	7 ± 6.6	0–44	15.3 ± 14.7	0–100
	Periphyton	15.9 ± 9.6	0–100	15.8 ± 13.8	0–100	15.2 ± 13.6	0–100	8.3 ± 7.5	0–52	15.3 ± 12.7	0–100
6	Forest leaf	10.5 ± 9.7	0–66	1.5 ± 2.0	0–10	/[a]		7.8 ± 7.3	0–46	1.6 ± 2.1	0–12
	C3 crop plant	9.8 ± 9.0	0–58	72.0 ± 3.3	0–82	/		42.7 ± 16.7	0–100	67.5 ± 3.3	58–78
	C4 crop plant	11.8 ± 10.8	0–74	2.6 ± 3.0	0–16	/		8.8 ± 8.2	0–50	2.8 ± 3.1	0–16
	Riparian plant	7.2 ± 6.9	0–48	2.4 ± 2.8	0–14	/		27.6 ± 14.8	0–80	2.4 ± 2.8	0–14
	Soil	29.1 ± 10.7	0–60	16.1 ± 3.2	0–22	/		3.5 ± 3.6	0–22	20.2 ± 3.2	0–26
	Organic fertilizer	21.1 ± 17.7	0–92	4.7 ± 4.9	0–26	/		5.1 ± 5.0	0–30	4.9 ± 5.0	0–26
	Periphyton	10.4 ± 9.3	0–58	0.6 ± 1.2	0–6	/		4.5 ± 4.6	0–28	0.6 ± 1.2	0–6
7	Forest leaf	10.5 ± 9.7	0–66	14.7 ± 13.0	0–86	9.8 ± 9.1	0–62	15.7 ± 13.9	0–98	13.8 ± 12.3	0–82
	C3 crop plant	9.8 ± 9.0	0–62	12.5 ± 10.4	0–52	9.1 ± 8.5	0–58	15.8 ± 13.2	0–72	12.7 ± 11.1	0–58
	C4 crop plant	11.8 ± 10.8	0–74	16.3 ± 14.4	0–98	11.0 ± 10.1	0–70	12.3 ± 11.0	0–78	15.2 ± 13.5	0–92
	Riparian plant	7.2 ± 6.9	0–48	11.0 ± 9.4	0–58	6.7 ± 6.4	0–44	29.9 ± 13.2	0–80	9.9 ± 8.8	0–58
	Soil	29.2 ± 10.7	0–60	12.9 ± 7.8	0–46	33.2 ± 10.7	0–62	3.8 ± 2.8	0–28	16.0 ± 8.6	0–48
	Organic fertilizer	21.1 ± 17.7	0–92	16.9 ± 13.0	0–70	20.6 ± 17.7	0–96	6.3 ± 6.1	0–42	18.6 ± 14.1	0–74
	Periphyton	10.4 ± 9.6	0–66	15.2 ± 13.0	0–86	9.7 ± 9.0	0–62	16.2 ± 14.1	0–100	13.7 ± 12.1	0–82
8	Forest leaf	15.1 ± 13.8	0–100	8.3 ± 7.8	0–50	12.4 ± 11.1	0–68	7.4 ± 7.2	0–48	10.4 ± 9.5	0–60
	C3 crop plant	10.3 ± 9.0	0–58	34.4 ± 20.9	0–100	39.5 ± 14.4	0–86	24.1 ± 17.0	0–100	40.3 ± 17.0	0–98
	C4 crop plant	15.0 ± 13.6	0–100	9.0 ± 8.4	0–54	14.2 ± 12.3	0–74	7.7 ± 7.5	0–50	11.6 ± 10.4	0–64
	Riparian plant	8.2 ± 7.0	0–44	34.1 ± 19.6	0–80	13.7 ± 9.3	0–40	47.8 ± 15.4	0–100	20.8 ± 13.0	0–54
	Soil	17.8 ± 13.5	0–76	3.7 ± 3.8	0–24	5.4 ± 5.2	0–32	3.3 ± 3.6	0–22	4.4 ± 4.5	0–28
	Organic fertilizer	17.1 ± 14.6	0–100	5.3 ± 5.2	0–32	7.9 ± 7.3	0–44	4.8 ± 4.9	0–30	6.5 ± 6.2	0–38
	Periphyton	16.5 ± 14.4	0–100	5.2 ± 5.1	0–32	6.9 ± 6.7	0–44	4.9 ± 4.9	0–30	6.0 ± 5.9	0–38

[a] No statistics were generated.

contrast, the low contributions of forest leaf and periphyton (e.g., values ranged from 9.8 ± 9.1% to 15.7 ± 13.9%) were not consistent with the characteristics of this Soyang Lake watershed, which is dominated by 80% of forested areas and a high autochthonous OM input (Namkung et al., 2001; Tenhunen et al., 2011).

3.4. Implications from the comparison of the two EMMA results

As shown in Tables 3 and 4, the estimated contributions based on the stable isotope ratios differ strongly from those based on fluorescence spectroscopy (Fig. 5). The most probable reason for this might be the limitation of the fluorescence characteristics of the AEOM among the diverse end member sources. Fluorescence spectroscopy has two major disadvantages concerning the capability for source apportionment. First, this tool is constrained to colored and fluorescent DOM only. The spectroscopic parameters are also subject to changes upon the occurrence of biogeochemical transformation, consequently affecting the source assignment (Derrien et al., 2017b; Yang and Hur, 2014).

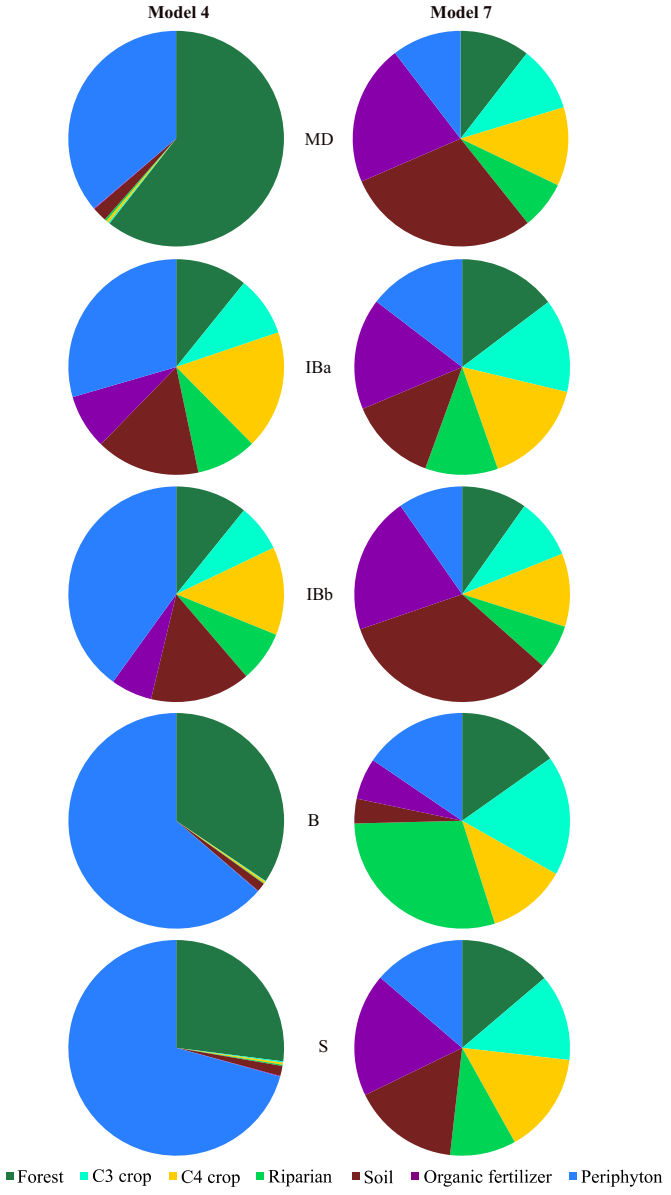

Fig. 5. Comparison of the EMMA results for source contributions to river sediments (i.e., SeOM) based on stable isotope ratios versus fluorescence parameters (Model 4 versus 7).

Furthermore, although the alkaline extraction method can be considered the most effective and more representative of POM than other mild extraction methods (Derrien et al., 2017a; He et al., 2016a; Hur et al., 2009; Rodriguez et al., 2014), the harsh alkaline treatment may alter the original optical signals of OM as it may break ester and amide bonds. It was previously reported that the method might preferentially extract the organic constituents associated with the origin of lignin or polyphenol (i.e., terrestrial sources) (Lehmann and Kleber, 2015). Some polyphenol compounds, such as tannins and lignans, also fluoresce in the peaks of tyrosine-like and tryptophan-like fluorescence, which makes it difficult to distinguish between terrestrial plants and algae (i.e., between allochthonous and autochthonous sources) (Beggs and Summers, 2011; Hernes et al., 2009; Maie et al., 2007). In the present study, the C2, which is assigned to protein-like component, was the most abundant component in all end-member samples. However, it could be assumed that the C2 component corresponds to a mixture of protein-like substances and polyphenol compounds. The preferential extraction of polyphenols would make the distinction between the two sources even more difficult.

The estimated source contributions based on the isotope ratios seem more consistent with the land use of the Soyang Lake watershed than those of the fluorescence parameters. Moreover, as the sample preparation for the isotope analyses does not modify the nature of the samples in contrast to the potential effect of harsh conditions during alkaline extraction, the EMMA based on the isotope ratios is likely to produce more reliable results.

4. Conclusions

The end-member modeling based on the isotopes showed relatively high contributions of terrestrial materials to the sediment (i.e., MD) heavily affected by forest and agricultural fields, while other sediments were characterized by a medium to a high contribution of periphyton with the values ranging from ~30% (IBa) to 70% (S). The EMMA based on fluorescence parameters, however, did not show similar results to that of the isotope ratios with low contributions exhibited for forest leaf and periphyton. The characteristics of the studied watershed were more consistent with the results based on the isotope ratios. The discrepancy in the EMMA capability for source assignments between the two analytical tools can be explained by the limited analytical window of fluorescence spectroscopy for non-fluorescent DOM and the inability of AEOM to represent the original bulk POM.

This study demonstrated the difficulty of quantifying the OM source contribution and confirmed the necessity of further efforts for better clarification in the future.

Acknowledgments

This work was supported by National Research Foundation of Korea (NRF) grants funded by the Korean government (MSIP) (No. 2017R1A4A1015393 and 2017033546). This work was additionally supported by the National Institute of Environmental Research R & D of Korea Government (NIER).

Appendix A. Supplementary data

Supplementary data to this article can be found online at https://doi.org/10.1016/j.scitotenv.2017.11.067.

References

Amiotte-Suchet, P., Linglois, N., Leveque, J., Andreux, F., 2007. 13C composition of dissolved organic carbon in upland forested catchments of the Morvan Mountains (France): influence of coniferous and deciduous vegetation. J. Hydrol. 335, 354–363.
Arnhold, S., Lindner, S., Lee, B., Martin, E., Kettering, J., Nguyen, T.T., Koellner, T., Ok, Y.S., Huwe, B., 2014. Conventional and organic farming: soil erosion and conservation potential for row crop cultivation. Geoderma 219–220, 89–105.

Barros, G.V., Martinelli, L.A., Oliveira Novais, T.M., Ometto, J.P.H.B., Zuppi, G.M., 2010. Stable isotopes of bulk organic matter to trace carbon and nitrogen dynamics in an estuarine ecosystem in Babitonga Bay (Santa Catarina, Brazil). Sci. Total Environ. 408, 2226–2232.
Beggs, K.M.H., Summers, R.S., 2011. Character and chlorine reactivity of dissolved organic matter from a mountain pine beetle impacted watershed. Environ. Sci. Technol. 45, 5717–5724.
Benner, R., Biddanda, B., Black, B., McCarthy, M., 1997. Abundance, size distribution, and stable carbon and nitrogen isotopic compositions of marine organic matter isolated by tangential-flow ultrafiltration. Mar. Chem. 57, 243–263.
Bianchi, T.S., Canuel, E.A., 2011. Chemical Biomarkers in Aquatic Ecosystems. Princeton University Press, Princeton University.
Briggs, R.A., Ruttenberg, K.C., Glazer, B.T., Ricardo, A.E., 2013. Constraining sources of organic matter to tropical coastal sediments: consideration of nontraditional end-members. Aquat. Geochem. 19, 543–563.
Burone, L., Muniz, P., Pires-Vanin, A.M.S., Rodrigues, M., 2003. Spatial distribution of organic matter in the surface sediments of Ubatuba Bay (Southeastern - Brazil). An. Acad. Bras. Cienc. 75, 77–80.
Carabel, S., Godínez-Domínguez, E., Verísimo, P., Fernández, L., Freire, J., 2006. An assessment of sample processing methods for stable isotope analyses of marine food webs. J. Exp. Mar. Biol. Ecol. 336, 254–261.
Choi, J., Kong, D.-S., Lee, H.-J., Park, S.-Y., Won, C.-H., Choi, Y., Lim, K.-J., 2010. Sediment Control Practices in Sloping Alpine Fields in Korea. 21st Century Watershed Technology: Improving Water Quality and Environment Conference Proceedings, 21–24 February 2010. Universidad EARTH, Costa Rica.
Coble, P.G., 2007. Marine optical biogeochemistry: the chemistry of ocean color. Chem. Rev. 107, 402–418.
Derrien, M., Cabrera, F.A., Tavera, N.L., Kantun Manzano, C.A., Vizcaino, S.C., 2015. Sources and distribution of organic matter along the Ring of Cenotes, Yucatan, Mexico: sterol markers and statistical approaches. Sci. Total Environ. 511, 223–229.
Derrien, M., Lee, Y.K., Park, J.E., Li, P., Chen, M., Lee, S.H., Lee, S.H., Lee, J.B., Hur, J., 2017a. Spectroscopic and molecular characterization of humic substances (HS) from soils and sediments in a watershed: comparative study of HS chemical fractions and the origins. Environ. Sci. Pollut. Res. Int. 24, 16933–16945.
Derrien, M., Yang, L., Hur, J., 2017b. Lipid biomarkers and spectroscopic indices for identifying organic matter sources in aquatic environments: a review. Water Res. 112, 58–71.
Dunn, R.J.K., Welsh, D.T., Teasdale, P.R., Lee, S.Y., Lemckert, C.J., Meziane, T., 2008. Investigating the distribution and sources of organic matter in surface sediment of Coombabah Lake (Australia) using elemental, isotopic and fatty acid biomarkers. Cont. Shelf Res. 28, 2535–2549.
Fichot, C.G., Kaiser, K., Hooker, S.B., Amon, R.M.W., Babin, M., Bélanger, S., Walker, S.A., Benner, R., 2013. Pan-Arctic Distributions of Continental Runoff in the Arctic Ocean. vol. 3 p. 1053.
Gao, X., Yang, Y., Wang, C., 2012. Geochemistry of organic carbon and nitrogen in surface sediments of coastal Bohai Bay inferred from their ratios and stable isotopic signatures. Mar. Pollut. Bull. 64, 1148–1155.
Goncalves-Araujo, R., 2016. Dissolved Organic Matter in Aquatic Systems: Assessment and Applications YOUMARES 7. 1, Hambourg. pp. 21–42.
Graeber, D., Gelbrecht, J., Pusch, M.T., Anlanger, C., von Schiller, D., 2012. Agriculture has changed the amount and composition of dissolved organic matter in Central European headwater streams. Sci. Total Environ. 438, 435–446.
Graham, M.C., Eaves, M.A., Farmer, J.G., Dobson, J., Fallick, A.E., 2001. A study of carbon and nitrogen stable isotope and elemental ratios as potential indicators of source and fate of organic matter in sediments of the Forth Estuary, Scotland. Estuar. Coast. Shelf Sci. 52, 375–380.
Guéguen, C., Cuss, C.W., Cassels, C.J., Carmack, E.C., 2014. Absorption and fluorescence of dissolved organic matter in the waters of the Canadian Arctic Archipelago, Baffin Bay, and the Labrador Sea. J. Geophys. Res. Oceans 119, 2034–2047.
He, W., Chen, M., Park, J.-E., Hur, J., 2016a. Molecular diversity of riverine alkaline-extractable sediment organic matter and its linkages with spectral indicators and molecular size distributions. Water Res. 100, 222–231.
He, W., Jung, H., Lee, J.-H., Hur, J., 2016b. Differences in spectroscopic characteristics between dissolved and particulate organic matters in sediments: insight into distribution behavior of sediment organic matter. Sci. Total Environ. 547, 1–8.
Hernes, P.J., Bergamaschi, B.A., Eckard, R.S., Spencer, R.G.M., 2009. Fluorescence-based proxies for lignin in freshwater dissolved organic matter. J. Geophys. Res. Biogeosci. 114 (n/a-n/a).
Huguet, A., Vacher, L., Relexans, S., Saubusse, S., Froidefond, J.M., Parlanti, E., 2009. Properties of fluorescent dissolved organic matter in the Gironde Estuary. Org. Geochem. 40, 706–719.
Hur, J., Williams, M.A., Schlautman, M.A., 2006. Evaluating spectroscopic and chromatographic techniques to resolve dissolved organic matter via end member mixing analysis. Chemosphere 63, 387–402.
Hur, J., Lee, D.-H., Shin, H.-S., 2009. Comparison of the structural, spectroscopic and phenanthrene binding characteristics of humic acids from soils and lake sediments. Org. Geochem. 40, 1091–1099.
Hur, J., Lee, B.-M., Lee, S., Shin, J.-K., 2014. Characterization of chromophoric dissolved organic matter and trihalomethane formation potential in a recently constructed reservoir and the surrounding areas – impoundment effects. J. Hydrol. 515, 71–80.
Inamdar, S., Singh, S., Dutta, S., Levia, D., Mitchell, M., Scott, D., Bais, H., McHale, P., 2011. Fluorescence characteristics and sources of dissolved organic matter for stream water during storm events in a forested mid-Atlantic watershed. J. Geophys. Res. Biogeosci. 116 (n/a-n/a).
Jørgensen, L., Stedmon, C.A., Kragh, T., Markager, S., Middelboe, M., Søndergaard, M., 2011. Global trends in the fluorescence characteristics and distribution of marine dissolved organic matter. Mar. Chem. 126, 139–148.
Jung, B.J., Lee, J.K., Kim, H., Park, J.H., 2014. Export, biodegradation, and disinfection byproduct formation of dissolved and particulate organic carbon in a forested headwater stream during extreme rainfall events. Biogeosciences 11, 6119–6129.
Jung, B.-J., Jeanneau, L., Alewell, C., Kim, B., Park, J.-H., 2015. Downstream alteration of the composition and biodegradability of particulate organic carbon in a mountainous, mixed land-use watershed. Biogeochemistry 122, 79–99.
Kim, H., Kaown, D., Mayer, B., Lee, J.-Y., Hyun, Y., Lee, K.-K., 2015. Identifying the sources of nitrate contamination of groundwater in an agricultural area (Haean basin, Korea) using isotope and microbial community analyses. Sci. Total Environ. 533, 566–575.
Lambert, T., Pierson-Wickmann, A.-C., Gruau, G., Thibault, J.-N., Jaffrezic, A., 2011. Carbon isotopes as tracers of dissolved organic carbon sources and water pathways in headwater catchments. J. Hydrol. 402, 228–238.
Lee, J.-Y., Kim, J.-K., Owen, J.S., Choi, Y., Shin, K., Jung, S., Kim, B., 2013. Variation in carbon and nitrogen stable isotopes in POM and zooplankton in a deep reservoir and relationship to hydrological characteristics. J. Freshw. Ecol. 28, 47–62.
Lee, Y., Hur, J., Shin, K.H., 2014. Characterization and source identification of organic matter in view of land uses and heavy rainfall in the Lake Shihwa, Korea. Mar. Pollut. Bull. 84, 322–329.
Lee, M.H., Payeur-Poirier, J.L., Park, J.H., Matzner, E., 2016. Variability in runoff fluxes of dissolved and particulate carbon and nitrogen from two watersheds of different tree species during intense storm events. Biogeosciences 13, 5421–5432.
Lehmann, J., Kleber, M., 2015. The contentious nature of soil organic matter. Nature 528, 60–68.
Lehmann, M.F., Bernasconi, S.M., Barbieri, A., McKenzie, J.A., 2002. Preservation of organic matter and alteration of its carbon and nitrogen isotope composition during simulated and in situ early sedimentary diagenesis. Geochim. Cosmochim. Acta 66, 3573–3584.
Maie, N., Scully, N.M., Pisani, O., Jaffé, R., 2007. Composition of a protein-like fluorophore of dissolved organic matter in coastal wetland and estuarine ecosystems. Water Res. 41, 563–570.
McCallister, S.L., Bauer, J.E., Cherrier, J.E., Ducklow, H.W., 2004. Assessing sources and ages of organic matter supporting river and estuarine bacterial production: a multiple-isotope (Δ14C, δ13C, and δ15N) approach. Limnol. Oceanogr. 49, 1687–1702.
McKnight, D.M., Boyer, E.W., Westerhoff, P.K., Doran, P.T., Kulbe, T., Andersen, D.T., 2001. Spectrofluorometric characterization of dissolved organic matter for indication of precursor organic material and aromaticity. Limnol. Oceanogr. 46, 38–48.
Meyers, P.A., 1994. Preservation of elemental and isotopic source identification of sedimentary organic matter. Chem. Geol. 114, 289–302.
Murphy, K.R., Butler, K.D., Spencer, R.G.M., Stedmon, C.A., Boehme, J.R., Aiken, G.R., 2010. Measurement of dissolved organic matter fluorescence in aquatic environments: an interlaboratory comparison. Environ. Sci. Technol. 44, 9405–9412.
Namkung, H., Kim, B.C., Hwang, G.S., Choi, K.S., Kim, C.G., 2001. Organic matter sources in a reservoir (Lake Soyang); primary production of phytoplankton and DOC, and external loading. Korean J. Limnol. 34, 166–174.
Ogrinc, N., Fontolan, G., Faganeli, J., Covelli, S., 2005. Carbon and nitrogen isotope compositions of organic matter in coastal marine sediments (the Gulf of Trieste, N Adriatic Sea): indicators of sources and preservation. Mar. Chem. 95, 163–181.
Osburn, C.L., Handsel, L.T., Mikan, M.P., Paerl, H.W., Montgomery, M.T., 2012. Fluorescence tracking of dissolved and particulate organic matter quality in a river-dominated estuary. Environ. Sci. Technol. 46, 8628–8636.
Phillips, D.L., 2001. Mixing models in analyses of diet using multiple stable isotopes: a critique. Oecologia 127, 166–170.
Phillips, D.L., Gregg, J.W., 2003. Source partitioning using stable isotopes: coping with too many sources. Oecologia 136, 261–269.
Phillips, D.L., Newsome, S.D., Gregg, J.W., 2005. Combining sources in stable isotope mixing models: alternative methods. Oecologia 144, 520–527.
Phillips, D.L., Inger, R., Bearhop, S., Jackson, A.L., Moore, J.W., Parnell, A.C., Semmens, B.X., Ward, E.J., 2014. Best practices for use of stable isotope mixing models in food-web studies. Can. J. Zool. 92, 823–835.
Rodriguez, F.J., Schlenger, P., Garcia-Valverde, M., 2014. A comprehensive structural evaluation of humic substances using several fluorescence techniques before and after ozonation. Part I: structural characterization of humic substances. Sci. Total Environ. 476-477, 718–730.
Ruddy, G., 1997. An overview of carbon and sulphur cycling in marine sediments. In: Rae, J.E., Jickells, T.D. (Eds.), Biogeochemistry of Intertidal Sediments. Cambridge University Press, Cambridge, pp. 99–118.
Santín, C., Yamashita, Y., Otero, X.L., Álvarez, M.Á., Jaffé, R., 2009. Characterizing humic substances from estuarine soils and sediments by excitation-emission matrix spectroscopy and parallel factor analysis. Biogeochemistry 96, 131–147.
Schindler Wildhaber, Y., Liechti, R., Alewell, C., 2012. Organic matter dynamics and stable isotope signature as tracers of the sources of suspended sediment. Biogeosciences 9, 1985–1996.
Stedmon, C.A., Bro, R., 2008. Characterizing dissolved organic matter fluorescence with parallel factor analysis: a tutorial. Limnol. Oceanogr. Methods 6, 572–579.
Stedmon, C.A., Markager, S., 2005. Resolving the variability in dissolved organic matter fluorescence in a temperate estuary and its catchment using PARAFAC analysis. Limnol. Oceanogr. 50, 686–697.
Stedmon, C.A., Markager, S., Bro, R., 2003. Tracing dissolved organic matter in aquatic environments using a new approach to fluorescence spectroscopy. Mar. Chem. 82, 239–254.
Tenhunen, J., Seo, B., Kim, I., Arnhold, S., Shope, C., Park, S.J., 2011. Spatial Setting of the TERRECO Project in the Soyang Lake Watershed of Gangwan-do and the Haean Catchment of Yanggu-gun. TERRECO Science Conference, Karlsruhe Institute of Technology, Garmisch-Partenkirchen, Germany.
Toming, K., Tuvikene, L., Vilbaste, S., Agasild, H., Viik, M., Kisand, A., Feldmann, T., Martma, T., Jones, R.I., Nõges, T., 2013. Contributions of autochthonous and allochthonous

sources to dissolved organic matter in a large, shallow, eutrophic lake with a highly calcareous catchment. Limnol. Oceanogr. 58, 1259–1270.
Torres, I.C., Inglett, P.W., Brenner, M., Kenney, W.F., Ramesh Reddy, K., 2012. Stable isotope (δ13C and δ15N) values of sediment organic matter in subtropical lakes of different trophic status. J. Paleolimnol. 47, 693–706.
Williams, C.J., Yamashita, Y., Wilson, H.F., Jaffé, R., Xenopoulos, M.A., 2010. Unraveling the role of land use and microbial activity in shaping dissolved organic matter characteristics in stream ecosystems. Limnol. Oceanogr. 55, 1159–1171.
Xiao, H.-Y., Liu, C.-Q., 2010. Identifying organic matter provenance in sediments using isotopic ratios in an urban river. Geochem. J. 44, 181–187.
Yamashita, Y., Boyer, J.N., Jaffé, R., 2013. Evaluating the distribution of terrestrial dissolved organic matter in a complex coastal ecosystem using fluorescence spectroscopy. Cont. Shelf Res. 66, 136–144.
Yang, L., Hur, J., 2014. Critical evaluation of spectroscopic indices for organic matter source tracing via end member mixing analysis based on two contrasting sources. Water Res. 59, 80–89.
Yang, L., Chang, S.-W., Shin, H.-S., Hur, J., 2015. Tracking the evolution of stream DOM source during storm events using end member mixing analysis based on DOM quality. J. Hydrol. 523, 333–341.
Yoon, S.-H., Kim, J.-H., Yi, H.-I., Yamamoto, M., Gal, J.-K., Kang, S., Shin, K.-H., 2016. Source, composition and reactivity of sedimentary organic carbon in the river-dominated marginal seas: a study of the eastern Yellow Sea (the northwestern Pacific). Cont. Shelf Res. 125, 114–126.
Yu, Z.T., Wang, X.J., Zhang, E.L., Zhao, C.Y., Liu, X.Q., 2015. Spatial distribution and sources of organic carbon in the surface sediment of Bosten Lake, China. Biogeosciences 12, 6605–6615.
Zsolnay, A., Baigar, E., Jimenez, M., Steinweg, B., Saccomandi, F., 1999. Differentiating with fluorescence spectroscopy the sources of dissolved organic matter in soils subjected to drying. Chemosphere 38, 45–50.

Supplementary Materials of

Estimation of different source contributions to sediment organic matter in an agricultural-forested watershed using end member mixing analyses based on stable isotope ratios and fluorescence spectroscopy

Morgane Derrien[a], Min-Seob Kim[b], Giyoung Ock[c], Seongjin Hong[d], Jinwoo Cho[a], Kyung-Hoon Shin[e,*] and Jin Hur[a,*]

[a] *Department of Environment and Energy, Sejong University, Seoul 143-747, South Korea*

[b] *Environmental Measurement & Analysis Center, National Institute of Environmental Research, Incheon 22689, South Korea*

[c] *National Institute of Ecology, Seocheon 33657, South Korea*

[d] *Department of Ocean Environmental Sciences, Chungnam National University, Daejeon, South Korea*

[e] *Department of Environmental Marine Sciences, Hanyang University, Ansan, Gyeonggi do 15588, South Korea*

* Corresponding author:

Tel. +82-2-3408-3826

Fax +82-2-3408-4320

E-Mail: jinhur@sejong.ac.kr

Tables: 5

Table S1. Detailed information on the sources samples from Soyang Lake watershed.

Source	Type	Location	Sample name
Forest leaf (n = 6)	Fallen leaf (wet)	Mandae (MD)	P1
	Fallen leaf (dry)		P2
	Fallen leaf (fresh)		P3
			P5
	Fallen leaf (fresh)	Buk (B)	P24
	Fallen leaf (dry)		P25
C3 crop plant (n=2)	Potato leaf	Haean basin	P7
	Rye leaf		P9
C4 crop plant (n=2)	Corn leaf	Haean basin	P8
	Corn leaf	Buk (B)	P26
Riparian plant (n=11)	Tall reed grass	Inbuk (IBb)	P10
	Mugwort leaf		P11
	Pussy willow leaf		P12
	Korean persicaria leaf		P13
	Tall reed grass	Soyang (S)	P14
	Mugwort leaf		P15
	Dock leaf		P17
	Pussy willow leaf	NaeRim	P19
	Dock leaf		P20
	Tall reed grass	Buk (B)	P21
	Pussy willow leaf		P22
Soil (n=7)	Ginseng field soil	Haean basin	S2
	Ginseng field soil		S3
	Potato field soil		S4
	Rye field soil		S5
	Corn field soil		S6
	Forest soil	Mandae (MD)	S8
	Forest soil		S9
Organic fertilizer (n=4)	Plant oilcake (Chamjoa Gold)	Haean basin	F5
	Commercial manure (Yanggu Agricultural Cooperative Federation)		F6
	Unknown composition		F7
	Cow manure		F9
Periphyton (n=4)	Unknown species	Inbuk (IBb)	A1
	Unknown species		A2
	Unknown species	Buk (B)	A3
	Unknown species		A4

Table S2. Identified components from the PARAFAC analysis.

Component	Excitation maxima (nm)	Emission maxima (nm)	Assignment	References	Tucker's Congruence Coefficients
C1	225, 340	434	Humic-like material	(Guéguen et al., 2014) (Jørgensen et al., 2011)	0.9804 0.9737
C2	220	326	Protein-like or tryptophan-like	(Dainard et al., 2015)	0.9567
C3	220, 310	434	Terrestrial humic-like	(Stedmon and Markager, 2005; Williams et al., 2010)	No match with OpenFluor
C4	220, 285	368	Protein-like and tryptophan-like, microbial-produced and possibly derived from aquatic production	(Graeber et al., 2012) (Williams et al., 2010)	0.9789 0.9721
C5	240, 275, 355	470	Humic-like, probably mixture of peak A and C (Coble, 1996)	(Yamashita et al., 2013)	0.9580

References

Coble, P.G. 1996. Characterization of marine and terrestrial DOM in seawater using excitation-emission matrix spectroscopy. Mar Chem 51, 325-346.

Dainard, P.G., Guéguen, C., McDonald, N., Williams, W.J. 2015. Photobleaching of fluorescent dissolved organic matter in Beaufort Sea and North Atlantic Subtropical Gyre. Mar Chem 177, Part 4, 630-637.

Graeber, D., Gelbrecht, J., Pusch, M.T., Anlanger, C., von Schiller, D. 2012. Agriculture has changed the amount and composition of dissolved organic matter in Central European headwater streams. Sci Total Environ 438, 435-446.

Guéguen, C., Cuss, C.W., Cassels, C.J., Carmack, E.C. 2014. Absorption and fluorescence of dissolved organic matter in the waters of the Canadian Arctic Archipelago, Baffin Bay, and the Labrador Sea. Journal of Geophysical Research: Oceans 119, 2034-2047.

Jørgensen, L., Stedmon, C.A., Kragh, T., Markager, S., Middelboe, M., Søndergaard, M. 2011. Global trends in the fluorescence characteristics and distribution of marine dissolved organic matter. Mar Chem 126, 139-148.

Stedmon, C.A., Markager, S. 2005. Resolving the variability in dissolved organic matter fluorescence in a temperate estuary and its catchment using PARAFAC analysis. Limnol Oceanogr 50, 686-697.

Williams, C.J., Yamashita, Y., Wilson, H.F., Jaffé, R., Xenopoulos, M.A. 2010. Unraveling the role of land use and microbial activity in shaping dissolved organic matter characteristics in stream ecosystems. Limnol Oceanogr 55, 1159-1171.

Yamashita, Y., Boyer, J.N., Jaffé, R. 2013. Evaluating the distribution of terrestrial dissolved organic matter in a complex coastal ecosystem using fluorescence spectroscopy. Cont Shelf Res 66, 136-144.

Table S3. Correlation and covariance of the isotopes dataset.

Correlation	$\delta^{13}C$ (‰)	$\delta^{15}N$ (‰)
$\delta^{13}C$ (‰)	1	
$\delta^{15}N$ (‰)	0.193	1
Covariance	$\delta^{13}C$ (‰)	$\delta^{15}N$ (‰)
$\delta^{13}C$ (‰)	19.821	
$\delta^{15}N$ (‰)	3.121	13.217

Table S4. Correlation and covariance of the five fluorescent components.

Correlation	C1 (%)	C2 (%)	C3 (%)	C4 (%)	C5 (%)
C1 (%)	1				
C2 (%)	-0.766	1			
C3 (%)	0.032	0.190	1		
C4 (%)	-0.301	-0.140	-0.830	1	
C5 (%)	-0.407	-0.032	-0.772	0.692	1
Covariance	C1 (%)	C2 (%)	C3 (%)	C4 (%)	C5 (%)
C1 (%)	61.678				
C2 (%)	-33.662	31.346			
C3 (%)	1.839	7.893	55.158		
C4 (%)	-13.586	-4.495	-35.406	33.011	
C5 (%)	-16.314	-0.924	-29.274	20.297	26.076

Table S5. Correlation and covariance of all the fluorescent parameters.

Correlation	C1 (%)	C2 (%)	C3 (%)	C4 (%)	C5 (%)	FI	HIX	BIX
C1 (%)	1							
C2 (%)	-0.766	1						
C3 (%)	0.032	0.190	1					
C4 (%)	-0.301	-0.140	-0.830	1				
C5 (%)	-0.407	-0.032	-0.772	0.692	1			
FI	0.158	-0.239	-0.379	0.231	0.307	1		
HIX	0.970	-0.665	-0.006	-0.357	-0.353	0.228	1	
BIX	-0.393	0.018	-0.907	0.921	0.861	0.298	-0.367	1
Covariance	C1 (%)	C2 (%)	C3 (%)	C4 (%)	C5 (%)	FI	HIX	BIX
C1 (%)	61.678							
C2 (%)	-33.662	31.346						
C3 (%)	1.839	7.893	55.158					
C4 (%)	-13.586	-4.495	-35.406	33.011				
C5 (%)	-16.314	-0.924	-29.274	20.297	26.076			
FI	0.099	-0.107	-0.225	0.106	0.125	0.006		
HIX	14.515	-7.099	-0.091	-3.904	-3.437	0.035	3.631	
BIX	-0.918	0.030	-2.005	1.575	1.309	0.007	-0.208	0.089